QEMF for spatial domain pre-processing in iris biometrics: advancing accuracy and efficiency in recognition systems

Prajwalasimha Sindugatta Nagaraja[1], Naveen Kulkarni[2], Raghavendra M. Ichangi[3], Vinitha Varanamkudath[2], Sharanabasappa Tadkal[2], Ranjima Parakkal[2], Deepthika Karuppusamy[2]

[1]School of Computing Science, Newcastle University (NUiS), Ang Mo Kio, Singapore
[2]Department of Computer Science and Engineering (Cyber Security), School of Engineering (SoE), Dayananda Sagar University, Bengaluru, India
[3]Department of Computer Science and Engineering - Data Science, Sphoorthy Engineering College, Hyderabad, India

Article Info

ABSTRACT

This article presents a Quantum-Enhanced Median Filtering (QEMF) method for spatial domain pre-processing in iris biometrics, designed to improve image denoising and recognition accuracy. Traditional median filtering often struggles with high noise density, leading to inconsistencies in the denoised image. Our approach enhances the median filtering process by integrating quantum-inspired principles with statistical measures, combining median and average values of neighboring pixels. This hybrid strategy preserves the structural integrity of the original image while effectively reducing noise. Additionally, a quantum-based thresholding step is introduced in the final stage to minimize ambiguities and further enhance image quality. The proposed method is evaluated using approximately one hundred standard iris images from the Chinese University of Hong Kong (CUHK) dataset, considering four types of noise: Impulse, Poisson, Gaussian, and Speckle. Comparative analysis with conventional filters, including Median and Wiener filters, demonstrates that the QEMF method achieves 99.36% similarity to the original images, surpassing Median and Wiener filters by 1.32% and 0.34%, respectively. These results highlight the potential of quantum-enhanced filtering for improved denoising performance and increased efficiency in iris recognition systems.

Corresponding Author:

Prajwalasimha Sindugatta Nagaraja
School of Computing Science, Newcastle University (NUiS)
Ang Mo Kio, Singapore 567 739, Singapore
Email: prajwalasimha.sn1@gmail.com

1. INTRODUCTION

Denoising of iris images typically involves applying various image processing techniques to remove noise and improve the clarity and quality of the iris image data. The denoising process is crucial in iris recognition systems because noise can distort the unique patterns of the iris, leading to errors in identification [1]-[3]. The iris is the circular, pigmented portion of the eye that surrounds the pupil and is visible through the transparent cornea. It serves both protective and optical functions and possesses unique and stable characteristics that are distinct for each individual. These characteristics can be reliably detected using near-infrared radiation, making iris recognition a robust biometric for verifying personal identity. The iris remains largely unchanged throughout a person's lifetime, which enhances its reliability as a biometric trait. Its distinct features and variations among individuals make iris recognition one of the most crucial methods for authenticating personal identity [4]-[7].

Iris recognition is highly valued for its stable and distinctive features, making it a reliable biometric for identity verification. Techniques such as frequency domain filters and binarization are utilized to enhance and simplify iris images for accurate recognition in various applications, from security systems to personal authentication [8]-[10]. The iris recognition system typically involves several stages: frequency domain filters are applied to enhance specific features of the iris image, often in the near-infrared spectrum. Subtraction process involves subtracting certain background elements or noise from the filtered image to isolate the iris's unique patterns. Despite the effectiveness of iris recognition, challenges can arise due to variations in imaging conditions, tissue characteristics, and structural components of the iris [11]-[13]. These challenges can lead to decreased performance in recognition accuracy, particularly when comparing to other methods like fingerprinting. To address some of these challenges, binarization is employed as an initial processing stage. Binarization simplifies the iris image by representing pixel values as either black or white (two saturation levels), focusing on preserving peak values that are crucial for recognition [14]-[18].

Iris recognition is extensively used for personal identity verification due to its reliability and uniqueness. It finds applications in both public sectors (e.g., border control and law enforcement) and private sectors (e.g., access control and financial transactions). Each individual's iris is unique, and iris recognition systems assign a unique label to each iris image to facilitate accurate identification. Pillai *et al.* [19] developed a system using nuclear technology for iris authentication. This system offers centralized authentication capabilities that can be integrated with multiple sensors. The centralized approach enhances efficiency and reduces costs by leveraging a single authentication system across various applications and locations. Tan and Kumar [20] proposed a framework that incorporates geometric information as a key coding technology for iris image recognition. Utilizing geometric features of the iris, such as the arrangement of ridges and other structural elements, enhances the recognition accuracy of the system. This approach improves upon traditional methods by incorporating additional discriminative features beyond pixel intensity and texture. Traditional iris recognition methods primarily focus on pixel intensity and texture analysis. Tan and Kumar [20] introduced the concept of incorporating geometric features of the iris. The combination of these characteristics allows for highly accurate and reliable identification and verification in iris recognition systems. Iris recognition is widely used in security applications due to its stability over time (the iris pattern remains relatively unchanged throughout a person's life) and its resistance to forgery or spoofing. By integrating geometric information into the recognition process, Tan and Kumar [20] aimed to improve accuracy beyond what can be achieved through pixel-based methods alone. Geometric features provide additional discriminative power, enabling more precise differentiation between similar iris patterns. Geometric features offer a richer set of discriminative attributes compared to pixel intensity and texture alone. These features are generally more stable and less affected by variations in illumination or image quality, which can be challenging for purely intensity-based methods. The incorporation of geometric information enhances overall system performance, leading to higher accuracy rates in identifying individuals based on their iris patterns.

The use of parabolic and clipped median filters in the rule matching approach [21] highlights their importance in enhancing the quality and reliability of iris images for subsequent recognition tasks. These filters exemplify critical preprocessing techniques aimed at optimizing the performance of iris recognition algorithms. Zhou and Sun [22] proposed a novel approach that integrates morphological analysis, pupil border histogram analysis, and external detection based on a boundary twice the size of the capillary. These methods work together to enhance overall accuracy. Another notable technology for iris recognition was introduced by Abidin [23], which utilizes several edge detection operators including Sobel, Prewitt, and Canny. These operators are employed to extract features from the iris, with particular emphasis on achieving enhanced results through the use of the Canny operator. Wang *et al.* [24] presented a method for improving iris recognition in noisy environments by employing the AdaBoost and the omnidirectional 2D Gabor filters as an integrated approach. Roy *et al.* [25] suggested that iris recognition can be impacted by various factors and proposed a method based on measuring the difference between pupils. They utilized Mumford-Shah segmentation to create distinct segments, aiming to mitigate these influences. The local binary pattern (LBP) model [26] extracts iris texture data in the form of patterns, integrates this with histogram attributes, and generates vectors to achieve accurate recognition. Alheeti [27] proposed a hybrid technology for iris recognition that focuses on enhancing the precision of edge detection. This approach aims to generate only the essential features necessary for accurate identification. Hussain [28] introduced an approach to extract location-specific markers from iris patterns. These markers were utilized to assess the performance of an iris recognition system under noise-free and noise-affected conditions. The evaluation involved using different sets of character vectors, specifically 4, 6, and 8, to analyze system performance.

The article proposes a quantum-enhanced median filtering (QEMF) method aimed at denoising process for iris images affected by noise. The prime objectives of the work are as follows: i) aims to reduce ambiguities and enhancing the quality of the denoised image by adjusting pixel values based on a specified threshold; ii) combines both median and average values of neighboring pixels and applying thresholding strategically, to

enhance image quality and fidelity; and iii) to design a hybrid approach to mitigate inconsistencies that can occur with standard median filtering, especially in regions with high noise density or significant pixel value variations.

In the proposed scheme, denoising is performed by modifying median filtering technique in spatial domain. The paper is organized as follows. Section 2 overviews method (filtering process). Performance analysis is tabulated in section 3. Final section concludes the article.

2.   METHOD

Sequential steps are considered for the filtering process. A predefined size (3×3) segment is considered inside which the center pixel is considered as the pixel of interest. Strong correlation in the adjacent pixels can be observed due to the grid nature of images [11]. Drastic change in the pixel value when compared with all the neighboring pixels in the segment leads to noise or other in-ambiguities associated with that pixel [11]. Comparison is made with respect to adjacent pixels to detect drastic changes in the pixel value due to noise. Corresponding median and average values are considered to restructure a noise-free image by a thresholding principle in the final stage of the algorithm. Figure 1 describes QEMF scheme for iris denoisification.
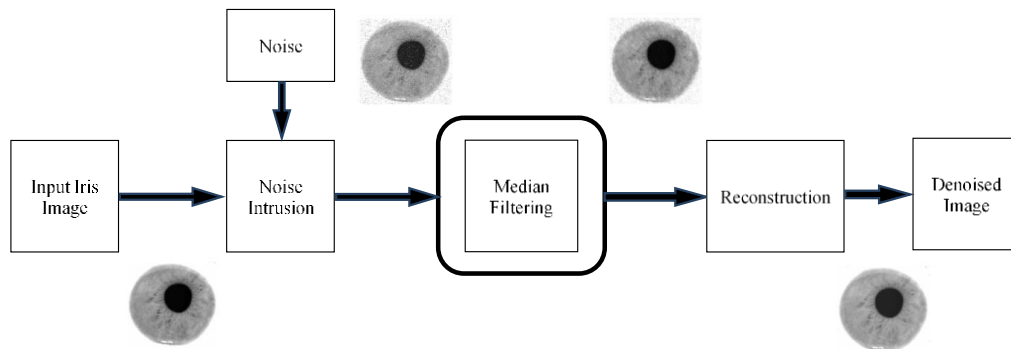

Figure 1. QEMF scheme

2.1. Filtering process using median filter

The process involves image processing, specifically concerning the computation of an effective median (M) using neighboring pixels in a 3×3 segment around a pixel of interest (p(x,y)).
− Pixel of interest (p(x,y)): this refers to a specific pixel in an image located at coordinates (x,y).
− Eight adjacencies: typically, this means considering the eight neighboring pixels surrounding the pixel of interest p(x,y). These neighbors are located to the north, south, east, west, and the four diagonal directions.
− Two medians for four adjacencies: this suggests that for the four orthogonal neighbors (north, south, east, west), two medians are computed. This could imply calculating the median of the four neighboring pixels separately for the north-south pair and the east-west pair.
− Difference computation: after computing the medians for the orthogonal pairs, the difference between these two median values is computed. This difference quantifies the variability or disparity between the two orthogonal sets of neighboring pixels.
− Average value of all elements in the segment (O): the segment O (1) refers to a 3×3 neighborhood around the pixel of interest p(x,y). This includes the pixel p(x,y) itself and its eight neighboring pixels (2). The average value of all these pixels in the 3×3 segment is computed.

$$O = \begin{bmatrix} p(x-1,y-1) & p(x,y-1) & p(x+1,y-1) \\ p(x-1,y) & p(x,y) & p(x+1,y) \\ p(x-1,y+1) & p(x,y+1) & p(x+1,y+1) \end{bmatrix} \tag{1}$$

− Effective median (M): finally, the effective median M is determined based on the computed differences between the orthogonal medians and the average value of the segment O. The exact formula or method to derive M from these components would depend on the specific algorithm or approach being used (3) and (4).

$$A = \frac{\sum_{1}^{total\ number\ of\ elements\ in\ the\ O}(O)}{total\ number\ of\ elements\ in\ the\ O} \tag{2}$$

$$M1 = \frac{p(x-1,y)+p(x+1,y)}{2} \tag{3}$$

$$M2 = \frac{p(x,y-1)+p(x,y+1)}{2} \tag{4}$$

Conditional statement involving two values, M1 and M2, compared to the value of 2 minus A. Original condition: {M1-A≥2-A}. This condition simplifies to M1≥2. If M1 is greater than or equal to 2, then the condition {M1-A≥2-A} will be true for any value of A. Action based on condition: if the condition {M1-A≥2-A} is true (meaning M1≥2), then you replace M by M2. Otherwise (if M1<2), replace M by M1.

```
Pseudo-code_1: if (M1 >=2) {
                    M=M2;
              } else {
                    M=M1;
              }
```

If M1 is greater than or equal to 2, assign M the value of M2. If M1 is less than 2, assign M the value of M1. This logic ensures that M (presumably a variable or value) is updated based on whether M1 meets the condition M1≥2 (Pseudo-code_1).

2.2. Filtering process using enhanced median filter

Describing a process involving image processing or reconstruction, where a derived segment (O') is created based on the difference between actual pixel values and a computed average value (A).
− Computed average value (A): a is the average value calculated from a set of pixel values, likely in a specific region or segment of an image.
− Actual pixel values: these are the original pixel values present in the image.
− Derived segment (O'): this refers to a new segment or image constructed based on the differences between the actual pixel values and the computed average value (A).
− Difference calculation: for each pixel in the segment O', the difference between the actual pixel value and the average value A is computed.
− Construction of O': O' is then reconstructed using these differences. The exact method of reconstruction could vary depending on the application, but typically, it involves modifying or transforming the original pixel values to reflect these differences (5).

$$O' = \begin{bmatrix} p(x-1,y-1)-A & p(x,y-1)-A & p(x+1,y-1)-A \\ p(x-1,y)-A & p(x,y)-A & p(x+1,y)-A \\ p(x-1,y+1)-A & p(x,y+1)-A & p(x+1,y+1)-A \end{bmatrix} \tag{5}$$

Describing a process where a derived median (M') is calculated based on certain rules involving a 3×3 segment (O') of an image. Derived segment (O'): this is a 3×3 segment (or neighborhood) extracted from the original image.
− Two medians for four adjacencies: within the 3×3 segment (O'), two medians are considered. This likely means that for the four adjacent pairs (horizontally and vertically adjacent pairs within the 3×3 grid), medians are computed separately.
− Difference calculation: the differences among these two medians are computed. This step helps quantify the variability or spread of values within the neighborhood.
− Average value calculation: an average value of all elements in the segment (O') is computed. This average likely serves as a reference or central value against which the differences are assessed.
− Effective derived median (M'): finally, the effective derived median (M') is defined based on the computed differences and the average value. The specifics of how M' is determined could involve rules such as selecting the median closest to the average, or adjusting based on the magnitude of differences computed earlier (6) and (7).

$$M1' = \frac{(p(x-1,y)+A)+(p(x+1,y)+A)}{2} \tag{6}$$

$$M2' = \frac{(p(x,y-1)+A)+(p(x,y+1)+A)}{2} \tag{7}$$

Describing a conditional statement involving two values, M1' and M2', compared to the value of 2' minus A. Original condition: {M1'-A≥2'+A}. This condition simplifies to M1'≥2'. If M1' is greater than or equal to 2', then the condition {M1'-A≥2'+A} will be true for any value of A. Action based on condition: If the condition {M1'-A≥2'+A} is true (meaning M1'≥2'), then you replace M' by M1'. Otherwise (if M1'<2'), you replace M' by M2'.

```
Pseudo-code_2: if (M1' >= 2') {
          M' = M1';
                  } else {
          M' = M2';
                  }
```

If M1' is greater than or equal to 2', assign M' the value of M1'. If M1' is less than 2', assign M' the value of M2'. This logic ensures that M' (the derived median or effective derived median in your context) is updated based on whether M1' meets the condition M1'≥2'. The values M1' and M2' likely represent different median calculations or adjustments based on the conditions and differences computed earlier in your image processing algorithm (Pseudo-code_2).

Comparison is made between the difference in the value of the pixel of interest ($p(x, y)$) with the average value (A) and predefined threshold. If the difference is more or less than the set threshold, pixel of interest is replaced by the difference value between the effective median (M) and the derived median (M'). Otherwise, pixel of interest ($p(x, y)$) is retained with its original value (Pseudo-code_3).

```
Pseudo-code_3: A = Compute_Average_Value_Around(p(x,y))
          diff = abs(p(x,y) + A)
          if diff > T:
                  diff_medians = abs(M - M')
                  p(x,y) = diff_medians
          else:
                  p(x,y) remains_unchanged
```

The replaced or retained pixel of interest is represented by D (8):

$$D = \begin{bmatrix} p(x-1,y-1) & p(x,y-1) & p(x+1,y-1) \\ p(x-1,y) & p'(x,y) & p(x+1,y) \\ p(x-1,y+1) & p(x,y+1) & p(x+1,y+1) \end{bmatrix} \tag{8}$$

3. RESULTS AND DISCUSSION

The proposed structured approach leverages standard test images, multiple performance metrics, and MATLAB for consistent, comprehensive, and reproducible evaluation. This methodology helps in understanding its strengths and potential areas for improvement compared to other spatial domain approaches. The study uses a set of 100 standard test images from the Chinese University of Hong Kong (CUHK). These images likely serve as a benchmark to evaluate the performance of various image processing techniques, including the proposed one. Five performance parameters (9) to (13) are considered, they are peak signal to noise ratio (PSNR), mean square error (MSE), mean correlation (NC), average difference (AD), and normalized average error (NAE) between host and the reconstructed images under four different noises. The overall average values of these performance parameters across the 100 iris images are computed and likely presented in graphical form (Figures 2 to 5). The comparison would typically include evaluating how the proposed technique fares under different types of noise conditions, ensuring robustness and general applicability.

$$MSE = \frac{1}{i*j} \sum_{x=1}^{i} \sum_{y=1}^{i} [O(i,j) - D(i,j)]^2 \tag{9}$$

$$PSNR = 10 \, log_{10} \left(\frac{i*j}{MSE} \right) \tag{10}$$

$$Correlation_{i,j} = \frac{cov(O,D)}{\sqrt{G(O)}\sqrt{G(D)}} \tag{11}$$

$$AD = \frac{1}{i*j} \sum_{x=1}^{i} \sum_{y=1}^{j} |D(i,j) - O(i,j)| \tag{12}$$

$$NAE = \frac{\sum_{x=1}^{i} \sum_{y=1}^{j} |D(i,j) - O(i,j)|}{\sum_{x=1}^{i} \sum_{y=1}^{j} |O(i,j)|} \tag{13}$$

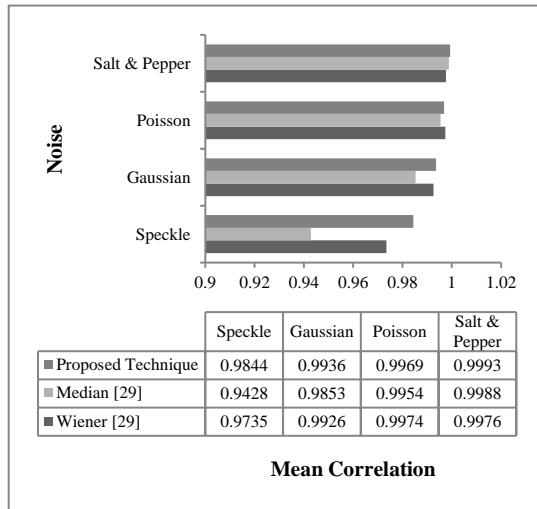where $O(i,j)$ is the original image and $D(i,j)$ is the denoised image.

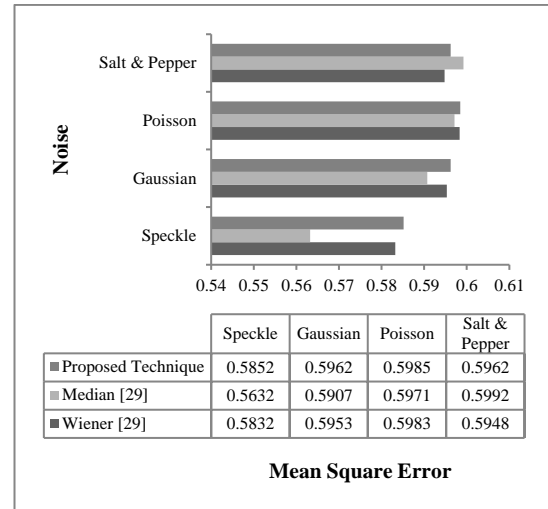Figure 2. Average NC of iris test images image
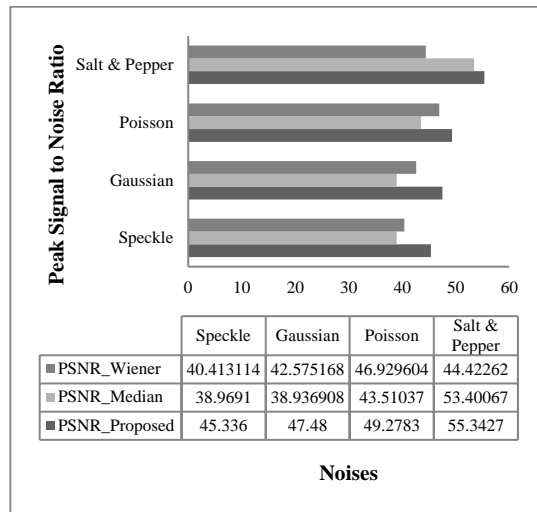

Figure 3. Average MSE of iris test images
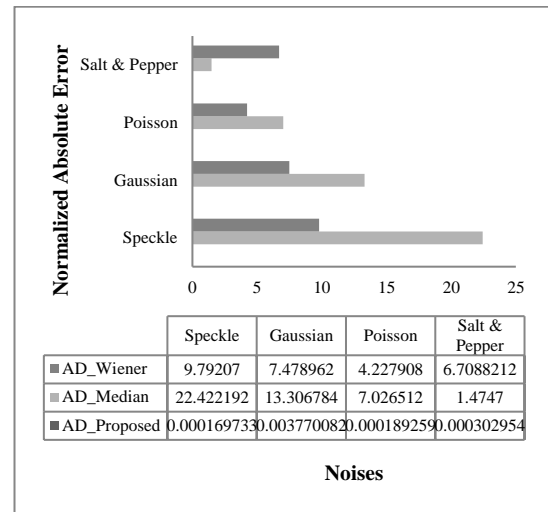

Figure 4. Average PSNR of iris test images images

Figure 5. Average NAE of iris test images

Figure 2 presents a comparison of the NC values obtained from the proposed technique and two other methods (Median filter and Wiener filter) across different types of noise (Salt and Pepper, Poisson, Gaussian, and Speckle). The proposed technique exhibits superior performance across all noise types based on the mean correlation metric, indicating its effectiveness in maintaining image quality. It outperforms the Wiener and Median filters, particularly excelling with Salt and Pepper noise. The Wiener filter is effective for Gaussian and Poisson noise but is less successful with Speckle, while the median filter is strong against Salt and Pepper noise yet lags with Gaussian noise. This analysis underscores the need for advanced algorithms tailored to specific noise types to achieve optimal image quality.

Figure 3 shows the comparison of MSE values for different noise reduction techniques (Median filtering and Wiener filtering.) applied to iris test images corrupted with various types of noise (Salt and Pepper, Poisson, Gaussian, Speckle). The Wiener filter performs reasonably well but shows slightly higher errors than the Median filter for all noise types. The proposed technique exhibits slightly higher MSE values than the Wiener and Median filters across the board, suggesting that while it may not minimize error as effectively, it could offer other advantages such as robustness or better handling of specific noise characteristics. Overall, the proposed technique is the most effective in terms of minimizing MSE for this dataset.

Based on the information provided about Figure 4, average PSNR for 100 sets of iris test images: The average PSNR across all noise types and possibly all filtering techniques is 49.35 dB. The PSNR values for the other technique are approximately 5.77 dB higher than those obtained with Wiener filtering. This comparison suggests that the unspecified noise reduction technique (possibly described earlier in Figure 4) achieves higher PSNR values (indicating better image quality in terms of noise reduction) compared to both Median and Wiener filtering techniques across various types of noise (Salt and Pepper, Poisson, Gaussian, and Speckle).

Based on the information provided about Figure 5, average normalized absolute error (NAE) for 100 sets of iris test images: the average value of NAE across all noise types and possibly all techniques is 12.54. The NAE values for the other technique are also lower compared to Wiener filtering, which has an NAE of 17.45.

4. CONCLUSION

The proposed QEMF method integrates median and average filtering with a quantum-inspired thresholding step to enhance image denoising in spatial domain pre-processing for iris biometrics. By addressing the limitations of traditional median filtering in high noise density scenarios, the approach ensures a more accurate approximation of pixel values. Evaluated on 100 images from the CUHK Iris dataset under Impulse, Poisson, Gaussian, and Speckle noise, the method demonstrated superior robustness, achieving 99.36% similarity with original images. This performance surpassed conventional Median and Wiener filters by 1.32% and 0.34%, respectively. The QEMF method effectively preserves image fidelity while reducing denoising errors, making it highly suitable for biometric authentication systems and medical imaging applications. Its ability to enhance recognition accuracy and processing efficiency ensures improved system reliability, contributing to more precise and secure iris recognition systems.

FUNDING INFORMATION

AUTHOR CONTRIBUTIONS STATEMENT

This journal uses the Contributor Roles Taxonomy (CRediT) to recognize individual author contributions, reduce authorship disputes, and facilitate collaboration.

Name of Author	C	M	So	Va	Fo	I	R	D	O	E	Vi	Su	P	Fu
Prajwalasimha Sindugatta Nagaraja	✓	✓	✓	✓	✓	✓	✓	✓	✓	✓	✓	✓	✓	✓
Naveen Kulkarni					✓				✓	✓	✓			✓
Raghavendra M. Ichangi					✓				✓	✓	✓			✓
Vinitha Varanamkudath					✓				✓	✓	✓			✓
Sharanabasappa Tadkal					✓				✓	✓	✓			✓
Ranjima Parakkal					✓				✓	✓	✓			✓
Deepthika Karuppusamy					✓				✓	✓	✓			✓

C	:	**C**onceptualization	I	:	**I**nvestigation	Vi	:	**Vi**sualization
M	:	**M**ethodology	R	:	**R**esources	Su	:	**Su**pervision
So	:	**So**ftware	D	:	**D**ata Curation	P	:	**P**roject administration
Va	:	**Va**lidation	O	:	Writing - **O**riginal Draft	Fu	:	**Fu**nding acquisition
Fo	:	**Fo**rmal analysis	E	:	Writing - Review & **E**diting			

CONFLICT OF INTEREST STATEMENT
Authors state no conflict of interest.

INFORMED CONSENT
We have obtained informed consent from all individuals included in this study.

DATA AVAILABILITY
Data availability is not applicable to this paper as no new data were created or analyzed in this study.

REFERENCES

[1]   Y. Dani and M. A. Ginting, "Comparison of Iris dataset classification with Gaussian naïve Bayes and decision tree algorithms," *International Journal of Electrical and Computer Engineering*, vol. 14, no. 2, pp. 1959–1968, 2024, doi: 10.11591/ijece.v14i2.pp1959-1968.
[2]   Y. I. Ibrahim and E. A. J. Sultan, "Iris recognition based on 2D Gabor filter," *International Journal of Electrical and Computer Engineering*, vol. 13, no. 1, pp. 325–334, 2023, doi: 10.11591/ijece.v13i1.pp325-334.
[3]   J. Wei, Y. Wang, Y. Li, R. He, and Z. Sun, "Cross-Spectral Iris Recognition by Learning Device-Specific Band," *IEEE Transactions on Circuits and Systems for Video Technology*, vol. 32, no. 6, pp. 3810–3824, 2022, doi: 10.1109/TCSVT.2021.3117291.
[4]   J. Wei, H. Huang, Y. Wang, R. He, and Z. Sun, "Towards More Discriminative and Robust Iris Recognition by Learning Uncertain Factors," *IEEE Transactions on Information Forensics and Security*, vol. 17, pp. 865–879, 2022, doi: 10.1109/TIFS.2022.3154240.
[5]   C. Wang, J. Muhammad, Y. Wang, Z. He, and Z. Sun, "Towards Complete and Accurate Iris Segmentation Using Deep Multi-Task Attention Network for Non-Cooperative Iris Recognition," *IEEE Transactions on Information Forensics and Security*, vol. 15, pp. 2944–2959, 2020, doi: 10.1109/TIFS.2020.2980791.
[6]   A. Rubio and B. Magnier, "Preprocessing of Iris Images for BSIF-Based Biometric Systems: Binary Detected Edges and Iris Unwrapping," *Sensors*, vol. 24, no. 15, p. 4805, 2024, doi: 10.3390/s24154805.
[7]   C. Wang and W. Zhang, "Image Global K-SVD Variational Denoising Method Based on Wavelet Transform," *Journal of Information Processing Systems*, vol. 19, no. 3, pp. 275–288, 2023, doi: 10.3745/JIPS.04.0277.
[8]   S. V. M. Sagheer and S. N. George, "A review on medical image denoising algorithms," *Biomedical Signal Processing and Control*, vol. 61, pp. 1–19, 2020, doi: 10.1016/j.bspc.2020.102036.
[9]   L. Fan, F. Zhang, H. Fan, and C. Zhang, "Brief review of image denoising techniques," *Visual Computing for Industry, Biomedicine, and Art*, vol. 2, no. 1, pp. 1–12, 2019, doi: 10.1186/s42492-019-0016-7.
[10]   S. Bian, X. He, Z. Xu, and L. Zhang, "Image Denoising by Deep Convolution Based on Sparse Representation," *Computers*, vol. 12, no. 6, pp. 112–125, 2023, doi: 10.3390/computers12060112.
[11]   R. Yan *et al.*, "Image Denoising for Low-Dose CT via Convolutional Dictionary Learning and Neural Network," *IEEE Transactions on Computational Imaging*, vol. 9, pp. 83–93, 2023, doi: 10.1109/TCI.2023.3241546.
[12]   D. H. Thai, X. Fei, M. T. Le, A. Zufle, and K. Wessels, "Riesz-Quincunx-UNet Variational Autoencoder for Unsupervised Satellite Image Denoising," *IEEE Transactions on Geoscience and Remote Sensing*, vol. 61, pp. 3291–3309, 2023, doi: 10.1109/TGRS.2023.3291309.
[13]   G. A. De Oliveira, L. M. De Almeida, E. R. De Lima, and L. G. P. Meloni, "Deep Convolutional Network Aided by Non-Local Method for Hyperspectral Image Denoising," *IEEE Access*, vol. 11, pp. 45233–45242, 2023, doi: 10.1109/ACCESS.2023.3273486.
[14]   A. E. Ilesanmi and T. O. Ilesanmi, "Methods for image denoising using convolutional neural network: a review," *Complex and Intelligent Systems*, vol. 7, no. 5, pp. 2179–2198, 2021, doi: 10.1007/s40747-021-00428-4.
[15]   K. Zhang, W. Zuo, Y. Chen, D. Meng, and L. Zhang, "Beyond a Gaussian denoiser: Residual learning of deep CNN for image denoising," *IEEE Transactions on Image Processing*, vol. 26, no. 7, pp. 3142–3155, 2017, doi: 10.1109/TIP.2017.2662206.
[16]   Z. Guo, Y. Sun, M. Jian, and X. Zhang, "Deep residual network with sparse feedback for image restoration," *Applied Sciences*, vol. 8, no. 12, pp. 1–10, 2018, doi: 10.3390/app8122417.
[17]   M. Elhoseny and K. Shankar, "Optimal bilateral filter and Convolutional Neural Network based denoising method of medical image measurements," *Measurement: Journal of the International Measurement Confederation*, vol. 143, pp. 125–135, 2019, doi: 10.1016/j.measurement.2019.04.072.
[18]   P. Kokil and S. Sudharson, "Despeckling of clinical ultrasound images using deep residual learning," *Computer Methods and Programs in Biomedicine*, vol. 194, pp. 1–8, 2020, doi: 10.1016/j.cmpb.2020.105477.
[19]   J. K. Pillai, M. Puertas, and R. Chellappa, "Cross-sensor iris recognition through kernel learning," *IEEE Transactions on Pattern Analysis and Machine Intelligence*, vol. 36, no. 1, pp. 73–85, 2014, doi: 10.1109/TPAMI.2013.98.
[20]   C. W. Tan and A. Kumar, "Efficient and accurate at-a-distance iris recognition using geometric key-based iris encoding," *IEEE Transactions on Information Forensics and Security*, vol. 9, no. 9, pp. 1518–1526, 2014, doi: 10.1109/TIFS.2014.2339496.
[21]   Y. Liu, F. He, X. Zhu, Y. Chen, Y. Han, and Y. Fu, "Video sequence-based iris recognition inspired by human cognition manner," *Journal of Bionic Engineering*, vol. 11, no. 3, pp. 481–489, 2014, doi: 10.1016/S1672-6529(14)60060-3.
[22]   S. Zhou and J. Sun, "A novel approach for code match in iris recognition," in *2013 IEEE/ACIS 12th International Conference on Computer and Information Science, ICIS 2013 - Proceedings*, 2013, pp. 123–128, doi: 10.1109/ICIS.2013.6607828.
[23]   Z. Z. Abidin, M. Manaf, A. S. Shibghatullah, S. Anawar, and R. Ahmad, "Feature extraction from epigenetic traits using edge detection in iris recognition system," *IEEE ICSIPA 2013 - IEEE International Conference on Signal and Image Processing Applications*, 2013, pp. 145–149, doi: 10.1109/ICSIPA.2013.6707993.
[24]   Q. Wang, X. Zhang, M. Li, X. Dong, Q. Zhou, and Y. Yin, "Adaboost and multi-orientation 2D Gabor-based noisy iris recognition," *Pattern Recognition Letters*, vol. 33, no. 8, pp. 978–983, 2012, doi: 10.1016/j.patrec.2011.08.014.
[25]   K. Roy, P. Bhattacharya, and C. Y. Suen, "Towards nonideal iris recognition based on level set method, genetic algorithms and adaptive asymmetrical SVMs," *Engineering Applications of Artificial Intelligence*, vol. 24, no. 3, pp. 458–475, 2011, doi: 10.1016/j.engappai.2010.06.014.
[26]   Rashad, Shams, Nomir, and El Awady, "IRIS Recognition Based On LBP and Combined LVQ Classifier," *International Journal*

of Computer Science and Information Technology, vol. 3, no. 5, pp. 67–78, 2011, doi: 10.5121/ijcsit.2011.3506.
[27]   K. M. Alheeti, "Biometric Iris Recognition Based on Hybrid Technique," International Journal on Soft Computing, pp. 1–9, 2011.
[28]   M. A. Hussain, "Eigenspace based accurate iris recognition system," in 2010 Annual IEEE India Conference (INDICON), 2010, pp. 1–3, doi: 10.1109/INDCON.2010.5712679.

BIOGRAPHIES OF AUTHORS

Dr. Prajwalasimha Sindugatta Nagaraja has introduced an innovative Chaotic System titled "n-Dimensional Multi-Linear Transformation (nD-MLT): Non-Linear Dynamics Application to Cryptography". He is a Postdoctoral Researcher at Newcastle University (NUiS), Singapore. He earned his Ph.D. in Cryptography and Cyber Security from Visvesvaraya Technological University, post-graduation from Regional Research Centre (RRC-VTU) in Digital Electronics and graduation from Visvesvaraya Technological University. Additionally, he has specialized in Cyber Security from New York University, USA. His research interests encompass nonlinear dynamics, chaos theory, cryptography, cyber security, IoT security, mathematical modeling, machine learning for cyber defence, and quantum cryptography. He can be contacted at email: prajwalasimha.sn1@gmail.com.

Naveen Kulkarni is working as Assistant Professor in the Department of Computer Science and Engineering (Cyber Security) at Dayananda Sagar University, Bangaluru. He received his post-graduation in Computer Science and Engineering from Visvesvaraya Technological University, India. His current area of research is Algorithm Optimization. His areas of interest include cloud computing, fog computing, computer algorithms, and edge computing. He can be contacted at email: naveenk-cse@dsu.edu.in.

Raghavendra M. Ichangi working as Assistant Professor in Computer Science and Engineering - Data Science at Sphoorthy Engineering College Hyderabad. He is M.Tech. graduate from National Institute of Technology Karnataka (NITK) Surathkal from the department of Computer Science and Engineering during the year 2013. His areas of interest include theory of computations, operating systems, operations research, optimization techniques, artificial intelligence, and machine learning. Presently he is pursuing Ph.D. in the area of Social Media Analytics from Visvesvaraya Technological University, India. He can be contacted at email: rmichangi@gmail.com.

Vinitha Varanamkudath is currently an Assistant Professor in Computer Science and Engineering (Cyber Security) Program at Dayananda Sagar University. She has completed her PG from Kannur University with Second Rank and UG from Calicut University. Pursuing her Ph.D. in Karpagam Deemed University. Her areas of interest include JAVA programming, computer architecture, python programming, cloud computing, app development, and cyber security. She can be contacted at email: vinitha.v-cs@dsu.edu.in.

Sharanabasappa Tadkal has completed his B.E. in Information Science and Engineering from Visvesvaraya Technological University. He has completed his M.Tech. in Computer Science and Engineering from Appa Institute of Engineering and Technology, Kalaburagi. And currently perusing Ph.D. at Vidhya Vardhaka College of Engineering-Research Center (VTU). Areas of interest include machine learning, artificial intelligence, threat hunting, detection and analysis, malware analysis, and forensics. He can be contacted at email: sharanabasappat-cse@dsu.edu.in.

Ranjima Parakkal obtained her Bachelor's and Master's degree in Computer Science and Engineering from Anna University, Chennai. Currently, pursuing her Ph.D. in the area of Cyber Security from Visvesvaraya Technological University, India. She has expertise in core subjects like computer networks, cryptography and network security, operating systems, and JAVA programming. She can be contacted at email: ranjimap-cse@dsu.edu.in.

Deepthika Karuppusamy obtained her Bachelor's and Master's degree in Computer Science and Engineering from Anna University, Chennai. Currently, pursuing her Ph.D. in the area of Blockchain Technology from Anna University, Chennai. She has expertise in core subjects like computer networks, cryptography and network security, blockchain technology, operating systems, and JAVA programming. She can be contacted at email: deepthika-cs@dsu.edu.in.